Hand Vein Biometry Based on Geometry and Appearance Methods

Aycan Yuksel*, Lale Akarun* and Bulent Sankur**

Abstract

Many biometric systems, such as face, fingerprint and iris have been studied extensively for personal verification and identification purposes. Biometric identification with vein patterns is a more recent approach that uses the vast network of blood vessels underneath a person's skin. These patterns in the hands are assumed to be unique to each individual and they do not change over time except in size. As veins are under the skin and have a wealth of differentiating features, an attempt to copy an identity is extremely difficult. These properties of uniqueness, stability and strong immunity to forgery of the vein patterns make it a potentially good biometric trait which offers greater security and reliable features for personal identification. In this study, we present a novel hand vein database and a biometric technique based on the statistical processing of the hand vein patterns. The BOSPHORUS hand vein database has been collected under realistic conditions in that subjects had to undergo the procedures of holding a bag, pressing an elastic ball and cooling with ice, all exercises that force changes in the vein patterns. The applied recognition techniques are a combination of geometric and appearance-based techniques and good identification performances have been obtained on the database.

Index Terms

Vein biometry, Hand vein database, Infrared imaging, BOSPHORUS hand vein database

I. Introduction

Developments in biometric technologies have achieved sufficiently high recognition rates under controlled conditions, but the need for reliability, robustness and convenience is still a major requirement that remains unfulfilled. Identification based on vein patterns emerges as a good candidate for a user friendly interface. Although there are already some studies regarding the uniqueness of vein patterns, the adversarial effects of temperature changes and various physical activities have not been considered. An important roadblock to the advancement of hand vein biometry is the lack of open hand vein databases, and hence, absence of reproducible results. Finally, there remains several new feature alternatives and feature/classifier fusion schemes that have not yet been explored. In this work, we intend to address all these three issues.

Anatomically, the shape of vascular patterns in the dorsal region of the hand is claimed to be unique to an individual even for identical twins [1], and it appears to remain stable over long periods of time. The structure of the vein patterns can be detected and captured with the help of infrared sensors. The visibility of the vein structure depends on various factors such as age, thickness of the skin, ambient temperature, physical activity, depth of the veins under the skin, to name a few. In addition, surface features such as moles, warts, scars and hair can also affect the imaging quality of the veins.

Identification using vein patterns is less studied compared to other human traits probably because the vein pattern is not observable under visible light. The structure of the vein patterns can be detected and captured with the help of infrared sensors. Typically, there are two kinds of imaging technologies, namely Far-infrared (FIR) and Near-infrared (NIR) imaging. FIR technology that works within the range 8-14 μm is more suitable for capturing the large veins in the back of the hand, but it is sensitive to ambient conditions and does not provide a stable image quality. On the other hand, NIR imaging that works within the range 700-1000 nm produces good quality images when capturing vein patterns in the back of the hand, palm, and wrist. This band is more tolerant to changes in

**B. Sankur is with the Department of Electric and Electronic Engineering, Bogazici University, Istanbul, Turkey e-mail: (bulent.sankur@boun.edu.tr)

*A. Yuksel and L. Akarun are with Department of Computer Engineering, Bogazici University, Istanbul, Turkey e-mails:(aycan.yuksel,akarun@boun.edu.tr)

[1]This work was funded by Bogazici University project 09HA202D and TUBITAK project 107E001

TABLE I
COMPARATIVE SURVEY OF METHODS

Reference	Data	Methods and Results
		Verification
C.-L. Lin *et al.* [13],	32 users, 30 samples/subjects, total 960 images	Multi-resolution analysis. $5\times$ enrollment. EER: 3.75
K. A. Toh *et al.* [5],	50 users, left and right hands, 10 samples/subjects, total 1000 images	Palm vein and palmprint scores are fused with SUM rule. SVM with RBF kernel is optimized for the vein features consisting of sub-sampled vein lines and for the directional wavelet energy features for palmprint. $5\times$ enrollment.
L. Wang *et al.* [3],	30 users, 9 samples/subjects, total 270 images	Vein images are skeletonized as in [17] and LEM is used. Triple enrollment. EER is claimed to be 0.
A. Kumar *et al.* [27],	100 users, 6 samples/subjects, total 600 images	EER is 1.14, EER of fusion is 0.38 for left hand and 0.28 for right hand.
		Identification
Y. Ding *et al.* [2],	48 users, 5 samples/subjects, total 240 images	The number of the end points and crossing points and the distances between them are used for feature extraction. Single enrollment. Identification rate: 99.1%.
Z. Wang *et al.* [4]	100 users, 5 samples/subjects, total 500 images	Single enrollment. Hausdorff, LEM and Gabor methods yield 58%, 66% and 80%, respectively.
A. Kumar *et al.* [28],	100 users, 6 samples/subjects, total 600 images	LRT, Hessian Phase, Ordinal Code and Laplacianpalm and their fusion is used. In single enrollment combined score is 96.67% for fusion (left hands). $3\times$ enrollment, 99.67%
This work	100 users, 3 samples/user, 4 conditions, total 1200 images	ICA, LEM and NMF methods as well as their fusion are considered. Identification rates are 94.16% for single enrollment and 97.33% for double enrollment.

environmental and body conditions, but it also faces the problem of disruption due to skin features such as hairs and line patterns [3].

L. Wang et al. [3] proposed a person verification system using the thermal-imaged vein pattern in the back of the hand based on the Line Segment Hausdorff Distance (LHD). They reported correct recognition of all subjects in a database of 30 persons. A. Kumar et al. [27] present a new technique based on shape features of knuckles based on minutiae matching of vein junction points. In a later paper, [28] Kumar and Prathyusha have used the fusion of Hessian phase and ordinal code, two different phase-based representations, namely, Laplacianpalm, which is an appearance based representation, and localized Radon transform, an orientation based representation. Z. Wang et al. [4] gave comparisons of shape and texture based methods for vein recognition. While shape similarity is measured via Hausdorff and Line Edge Map (LEM), texture similarity was measured via Euclidean distance of Gabor magnitude features. In a dataset of 100 persons, Hausdorff, LEM and Gabor based methods achieved accuracies of 58%, 66% and 80%, respectively. C.-L. Lin et al. [13] presented person verification results using hand dorsal images acquired from IR images in the 3.4 - 5 μm band. Their approach is based on the combination of multiresolution images obtained from the pre-processed thermal vein images. G. Wang et al. [14] proposed a multimodal person identification system where palmprint and palm vein modalities were combined in a single image. Locality Preserving Projection (LPP) was used to extract features of the fused images and they called this "Laplacianpalm". A summary of literature is presented in Table I. In this table, the second column gives the database information, such as the gallery size, the enrollment size, and the total number of images; specifically, $5\times$ enrollment refers to 5 images per subjects in the enrollment set.

Reproducibility of results is an essential requirement for the advancement of a technology. Although there is an increasing number of papers that report good recognition results, none of them allow open access to their database; hence their results are not reproducible. Thus in our study, we collected a hand vein database, called BOSPHORUS, which is open access to researchers (http://bosphorus.ee.boun.edu.tr/). The rest of the paper is organized as follows. Section II gives the details of the hand-vein database. In Section III we discuss feature alternatives for hand vein biometry, and in Section IV we present classification and classifier fusion issues. Experimental results are presented in Section V, and finally, conclusions are drawn in Section VI.

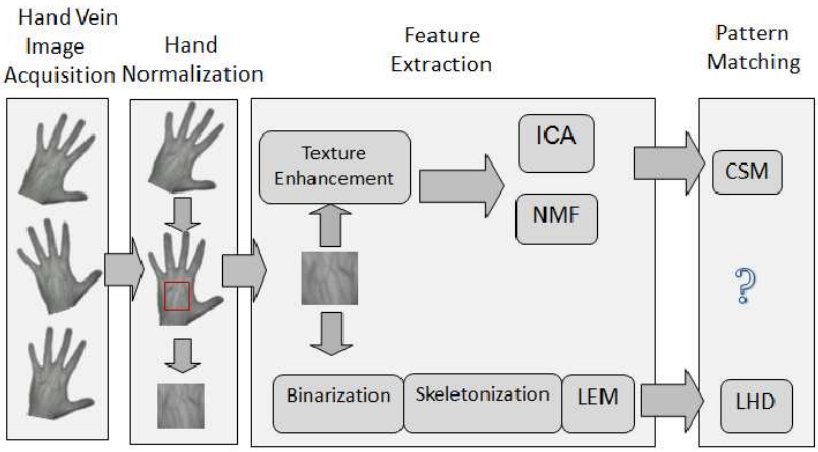

Fig. 1. Block diagram of the hand vein biometry system. (ICA: Independent Component Analysis, NMF: Non-negative Matrix Factorization, CSM: Cosine Similarity Measure, LEM: Line Edge Map, LHD: Line Segment Hausdorff Distance)

II. Bosphorus Hand Vein Database

The hand vein biometric identification system consists of four main processing stages: I) image acquisition, II) hand normalization, III) feature extraction, IV) matching and identity detection; as shown in Figure 1. In this section, we give details about image acquisition, data collection, and hand normalization.

A. Image Acquisition and Camera Setup

NIR imaging technology and reflection method have been chosen for image acquisition. A monochrome NIR CCD camera (WAT-902H2 ULTIMATE [8]) fitted with an infrared lens is used to capture the vein patterns in the back of the hand. This camera has a good sensitivity in the near infrared spectrum (Figure 2(b)). The region of interest is irradiated by two IR light sources. Light sources are composed of six infrared LEDs which are placed in a circular combination. Diffusing papers are placed in front of the infrared light sources to scatter the light uniformly. In order to eliminate the effects of visible light, the setup is installed in a dark room. In a real-life acquisition set-up, the access location will not be dark, but the device enclosure will control and limit substantially the amount of interfering visible light. The camera in the overhead position is adjusted approximately 80 cm above the hand stand. Users were asked to place their hands on a black background with the back of the hand facing the camera. The images were digitized into 640×480 pixels with a gray-scale resolution of 8-bit per pixel and after deinterlacing, the image size was reduced to 300×240 pixels. Our hand vein database contains 1200 images of left hands of 100 different people. Each subject underwent four imaging sessions that consisted of the left hand

- Under normal condition (N: Normal),
- After having carried a bag weighing 3 kg. for one minute (B: Bag),
- After having squeezed an elastic ball repetitively (closing and opening) for one minute (Activity: A),
- After having cooled the hand by holding an ice pack on the surface of the back of the hand (Ice: I).

These sessions intend to simulate physical stress conditions that could occur in real-life are denoted by the mnemonic symbols N, B, A, I, corresponding to normal conditions, bag carrying exercise, ball pressing exercise and cooling with ice. In each session we captured three images, which resulted in $3 \times 4 = 12$ images per subject of his left hand under four different conditions. The subjects (100 people, 42 female and 58 male) were volunteers chosen from undergraduate students, staff and administrative members from a large age bracket. The histogram of the age distribution of the subjects is given in Figure 3. In addition to the left hand images, we collected 300 right hand images from subjects under normal conditions. The right hand data is intended to test the degree of interchangeability between left and right hands, or to investigate the performance if both hands were presented. Finally, since any biometric system should pass the test of time lapse, we collected additional data of left hands under normal conditions from 25 persons after some time ranging from two months to five months. For each individual, we also recorded demographic information. The database is presently open access at http://bosphorus.ee.boun.edu.tr/

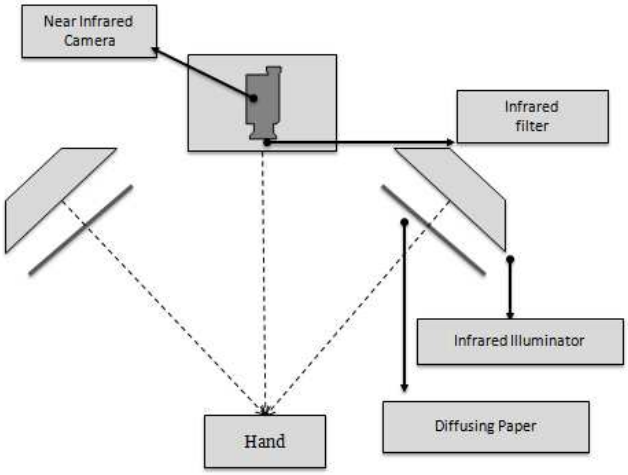

(a) Camera Setup

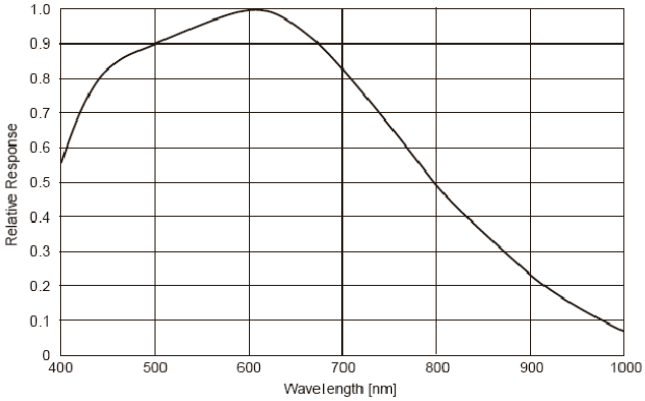

(b) Camera Response

Fig. 2. (a) The hand vein image acquisition setup (b) Acquisition camera's spectral response

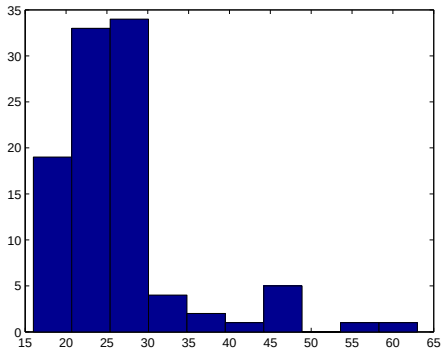

Fig. 3. Age histogram of the database

TABLE II
DATABASE INFORMATION

Gender	Female: 42 persons, Male: 58 persons
Left/Right Handed	Left: 2 persons, Right: 98 persons
Age	Varying between 16-63

Fig. 4. Hand vein images of two different subjects and their region of interest using Yoruk's hand normalization process [6], [7]

B. Normalization of Hand Images

In order to match hand veins correctly, pose and posture normalizations are necessary. Hand images captured in arbitrary poses and postures are brought to standard finger orientations and pose, using the normalization algorithm proposed by Yoruk et al. [6], [7]. Yoruk's algorithm starts with K-means clustering (K=2), to extract the hand from the background, followed by morphological filtering to fill in holes. This stage yields the silhouette of the hand. This is followed by several processing steps, namely, hand rotation and translation, finding the finger axes and tips, removal of ring artifacts, completion of the wrist, estimation of finger pivots and translation of fingers to standard orientations. The region of interest (ROI) is defined as the 100×100 image patch extracted from the center of the palm region (Figure 4).

III. Feature Extraction

We have extracted features from images of hands using both appearance-based methods and methods reflecting the hand geometry. The appearance-based methods consider the dorsal view of the hand in the near infrared band and project it to subspaces via Independent Component Analysis (ICA) or Non-negative Matrix Factorization (NMF) methods. The geometry-based method delineates the veins via skeletonization and then describes the vein structure as a graph.

While the LEM features are vein-oriented, subspace-based features are appearance descriptors. The advantages of subspace-based features is that they are generative and simple to characterize. Furthermore, they yield a plausible distance measure when one tries to reconstruct a hand vein image from its subspace. The common appearance-based features are PCA (Principal Component Analysis), LDA (Linear Discriminant Analysis), ICA, NMF and their kernelized versions. In this work, we opted for the ICA and NMF variety based on our previous successful experience in face recognition [25] and hand shape recognition [26]. Other interesting classes of features could be local features tailored to hand images. Examples of such local features are Gabor wavelets, local binary patterns (LBP), SIFT (Scale Invariant Feature Transform) feature descriptors, and gradient field. When these features are treated along their spatial coordinates, they become capable of representing both local properties and their configurational information.

We give details of the chosen ICA, NMF and LEM methods below.

A. ICA Features

Independent Component Analysis (ICA) is a technique for extracting statistically independent variables from a mixture of them. There exist two possible formulations of ICA. In the first architecture, called ICA1, each of N individual hand-data vectors is assumed to be a linear mixture of an unknown set of N statistically independent source hands. Thus the observed signals (hand images) $\{x_i(k), k = 1, .., K\}$, $i = 1, .., N$ are a mixture of a set of N unknown independent source signals s_i which are linearly combined through an unknown mixing matrix A and where K denotes the vector size corresponding to the number of pixels. This results in the model:

$$X = AS \tag{1}$$

where, x_i and s_i are rows of a N x K matrix. In the second architecture, ICA2, the superposition coefficients are assumed to be statistically independent, but not the basis images. Accordingly, each of K pixels of the hand images result from independent mixtures of random variables. Eq. 1 still holds but x_i and s_i form columns of a $K \times N$ matrix. The data vectors fed into the ICA analysis are the lexicographically ordered hand image pixels. The dimension of these vectors is K = 10000, for our region of interest of size 100×100 in vein images. Briefly, ICA aims to find a linear transformation W, also called separating or de-mixing matrix, for the inputs that minimize the

TABLE III
COMPARISON OF BINARIZATION METHODS (ME: MISCLASSIFICATION ERROR, MHD: MODIFIED HD; SEE [10] FOR THE DETAILS OF THE PERFORMANCE METRICS)

	Accuracy	ME	Hausdorff	MHD
Niblack	0.69	0.30	15.85	1.16
Bernsen	0.86	0.13	15.03	0.41
Yasuda	0.94	0.05	12.31	0.27
Wang [3]	0.74	0.25	14.86	0.81
Otsu	0.78	0.21	29.65	2.04

statistical dependence between the output components, the latter being estimates of the hypothesized independent sources s_i:

$$S \cong WX \tag{2}$$

We implemented Eq. 2 via fastICA algorithm [11]. Fig. 8 shows the plot of the histograms of the intra-subject (genuine-to-genuine) differences and of the inter-subject differences (genuine-to-impostor) for ICA1 features.

B. NMF Features

Non-negative Matrix Factorization (NMF) is another matrix factorization technique with the added constraint that each factor matrix must have only non-negative coefficients [15], though statistical independence is not sought for. Given a non-negative data matrix X (as in Eq. 1 and 2) of size $K \times N$, we obtain two non-negative matrices W and H such that:

$$X \cong WH \tag{3}$$

where W is of size $K \times L$ and H of size $L \times N$. Since we force the two matrices to be non-negative, we can only reconstruct X approximately from their product. The columns of W can be regarded as basis vectors and the columns of H are utilized as feature vectors of the corresponding vein images. We use Hoyer's code [16] for NMF representation.

C. LEM Features

Line Edge Map (LEM) is an approach that extracts lines from an image edge map as features. The algorithm can be considered as a combination of template matching and geometrical feature matching. It was proposed by Gao and Leung [9] for face recognition and then applied to vein biometry by Wang et al. [3]. The steps of binarization, skeletonization and line extraction as adapted to vein images are detailed below. The basic unit of LEM is the line segment grouped from pixels of the edge map and matching of line segments is based on the Line Segment Hausdorff Distance (LHD). Two image patterns are considered to be similar if their LHD is small.

The LEM algorithm starts with thresholding and segmenting the foreground (vein) regions. This is followed by morphological noise filtering and skeletonization, which finally yield the vein line segments. Once the hand images are reduced to vein skeletons, the recognition will be based on some measure of line graph similarity. Gao and Leung [9] extend the concept of Hausdorff distance into LHD to compare line patterns. Briefly LHD incorporates structural information of line segment orientations, line lengths and line-point associations.

1) Image Binarization: We have compared several binarization methods. Global thresholding of NIR images does not always prove to be successful; hence, we resort to local binarization methods such as Yasuda [10], Bernsen [10], Niblack [10], Wang [3]. For comparison we also include one global method, Otsu [10]. Based on several ground truth-images the scores of various similarity criteria [10], such as accuracy, misclassification error (ME), Hausdorff distance and Modified Hausdorff Distance (MHD) between ground-truth images and test images are shown in Table III. The best results have been obtained with the Yasuda method.

In the Yasuda method [10] one first applies a normalization process, followed by a nonlinear smoothing, which preserves the sharp edges and culminating in an adaptive thresholding and segmentation stage. Finally noise filtering and skeletonization yield the vein line segments.

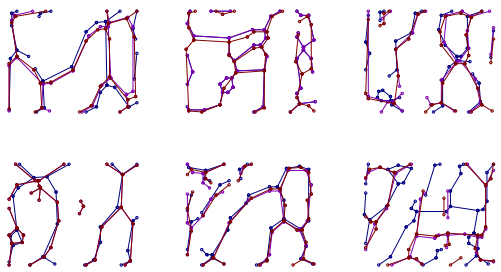

Fig. 5. Three LEMs of the users are displayed with different colors on the same figure in order to show the variations.

Fig. 6. LEM extraction steps: (left-to-right) A vein image, Yasuda binarization, noise removal, skeletonization and line segments generation

2) LHD: While Hausdorff distance is a natural measure for comparing similarity of sets and shapes, its extension called LHD is a measure to compare line patterns. LHD incorporates structural information of line segment orientations and line-point associations, and hence is effective in comparing two shapes made up of a number of curve segments.

LHD measures the degree of dissimilarity between two LEMs. LEM is a representation which records only the end points of line segments on curves. Given two LEMs, $M^l = \{m_1^l, m_2^l, .., m_p^l\}$ representing a model in the database and $T^l = \{t_1^l, t_2^l, .., t_q^l\}$ representing a test input LEM where the superscript l stands for line, $\vec{d}(m_i^l, t_j^l)$ represents the dissimilarity defined as:

$$\vec{d}(m_i^l, t_j^l) = \begin{bmatrix} d_\theta(m_i^l, t_j^l) \\ d_\parallel(m_i^l, t_j^l) \\ d_\perp(m_i^l, t_j^l) \end{bmatrix} \tag{4}$$

where $d_\theta(m_i^l, t_j^l)$, $d_\parallel(m_i^l, t_j^l)$ and $d_\perp(m_i^l, t_j^l)$ are the angular distance, parallel distance and perpendicular distance, respectively. Using these distances, LHD has been calculated using the equations defined in [9]. LHD steps are

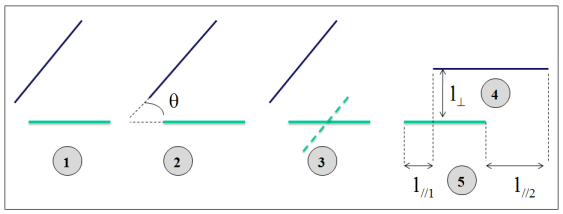

Fig. 7. Illustration of the LHD calculation: 1) Two line segments; 2) Angular distance, 3) Rotation of the shorter segment for parallelism; 4) Paralel distance, $l_{\parallel 1}$; 5) perpendicular distance, $l_\perp$

given in Figure 7.

Three different LEMs of the same person are superimposed in Figure 5. There are registration problems, sometimes because of the normalization process, sometimes because of the binarization or skeletonization process, as well as because of the acquisition conditions.

IV. Feature Matching and Classifier Fusion

In the identification mode, the user does not provide any identity claim, but the system must find out the user's identity from a database of enrolled users. For the person identification task, we measure the distance between

TABLE IV
IDENTIFICATION AND VERIFICATION (EER) RESULTS FOR SINGLE-ENROLLMENT, NAIVE TESTS

Test Set		ICA1	ICA2	NMF	LEM
Normal	Iden.Rate:	88.66	**94.16**	81.33	68.5
	EER:	4.02	**2.47**	8.14	13.52
Bag	Iden.Rate:	**78.33**	72.33	71.44	73.77
	EER:	**8.01**	13.04	12.77	12.13
Activity	Iden.Rate:	**75.55**	68.88	68.88	71.77
	EER:	**9.20**	13.23	14.11	12.76
Ice	Iden.Rate:	**68.77**	64.88	66.55	65.77
	EER:	**11.52**	14.88	15.08	14.07
All	Iden.Rate:	**77.82**	75.06	72.06	69.95
	EER:	**8.18**	10.90	12.53	13.12

TABLE V
IDENTIFICATION AND VERIFICATION (EER) RESULTS FOR DOUBLE-ENROLLMENT, NAIVE TESTS

Test Set		ICA1	ICA2	NMF	LEM
Normal	Iden.Rate:	94.33	**97.33**	89.67	81.66
	EER:	2.43	**1.53**	4.00	7.41
Bag	Iden.Rate:	**88.55**	82.88	83.33	88.44
	EER:	**4.75**	8.69	7.33	7.33
Activity	Iden.Rate:	**86.44**	79.44	81.89	**86.66**
	EER:	**6.22**	8.00	8.33	6.47
Ice	Iden.Rate:	77.66	74.77	77.22	**80.77**
	EER:	**8.22**	10.76	10.89	9.13
All	Iden.Rate:	**86.74**	83.60	83.03	84.38
	EER:	**5.40**	7.24	7.64	7.59

the test feature vector and all the feature vectors in the database belonging to N different subjects. For a person verification task, one must differentiate the genuine hand from the impostor (in our context, everybody else in the database) hands as the user provides her hand image in support of her claimed identity. For this purpose, the distances between the hand of the applicant and all the hands in the database are calculated and the scores are compared against a threshold.

For ICA and NMF techniques, L1 (mean absolute difference), L2 (Euclidean) and CSM (cosine similarity measure) were compared and the best results have been obtained with CSM, calculated as:

$$d_{cos}(a_i, a_{test}) = \frac{a_i \cdot a_{test}}{\|a_i\| \, \|a_{test}\|} \tag{5}$$

We have considered four fusion techniques to improve the performance of the individual schemes used for the identification and verification tasks. We have used the Borda count technique, majority voting, which is a decision level fusion technique, and three score fusion techniques: product rule, sum rule, and weighted sum rule [12].

a) Borda Count: Each classifier outputs a rank, and the ranks from individual classifiers are summed and the identity of the vein pattern is declared to be the one with the lowest sum rank.

b) Majority Voting: Each classifier casts a vote of 1 to a class if the test pattern belongs to that class. The class having the highest vote is declared to be the identity of the pattern.

c) Z-score Normalized Product: Each classifier produces a similarity value from the test image to the classes. The values are mapped to the range [0, 1] with z-score normalization. Normalized scores are multiplied to obtain the final score.

d) Z-score Normalized Sum: After z-score normalization, the scores are summed up to obtain the final score.

e) Z-score Normalized Weighted Sum: Sum Rule is actually a special case of weighted sum with equal weights. We have experimented with different weights. As expected, giving more weight to the better performing classifier yielded better results. Accordingly, we assigned the following weights: 0.6 for ICA1, 0.2 for LEM and 0.2 for NMF.

V. Experimental Results

We have performed our experiments on the BOSPHORUS hand vein database described in Section II. To describe the different experiments, we use the following short-hand notation: A-to-B test means that in the experiment the training set was A and the test set was B; furthermore we denote as "naive test" the case when the training set consists only of the N set, and the "informed test" denotes the case when all conditions are represented in the training set. Thus, for example, N-to-N denotes training and naive testing with normals (e.g. first row of Tables IV and V); N-to-NBAI means training with N and naive testing with all N, B, A and I conditions, and NBAI-to-NBAI corresponds to "informed testing" with all N, B, A and I conditions.

We use paired t-test to compare the accuracies for statistically significant difference. At a significance level of five percent the paired t-test confirmed that the algorithms are statistically different for individual test sets. Naturally the training and test image sets are disjoint in all experiments.

For the sake of clarity, we give the following details about our experiments. In the naive experiments, the training set consists of normals (N), while there are five test set cases, namely, N, I, A, B and the union of all the four sets. The results of naive experiments are given in Tables IV, V, VII, VIII. In the informed experiments, the training sets consist of the union of all four sets, and the test sets again consist of the five cases, N, I, A, B and, the union of all the four sets. Finally, since three palm vein images were captured per N, B, A and I condition, this gave us three session rounds in each case. More explicitly, let us denote these images as 1, 2 and 3. In the single enrollment case, the training and testing combinations were (1, (2,3)), (2, (1,3)), (3,(1,2)); in the double enrollment case, the training and testing combinations were ((1, 2), 3), ((1,3), 2), ((2,3), 1). We report in the tables the average of these three rounds.

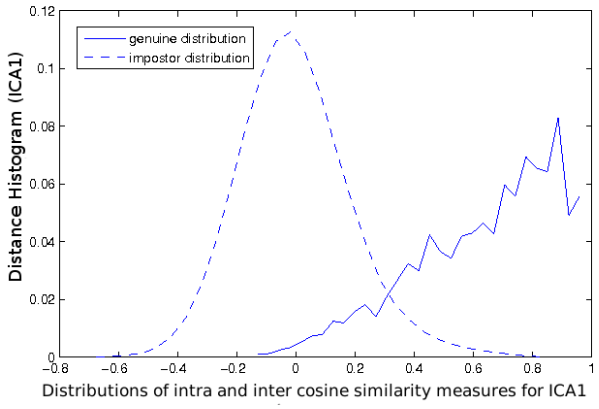

Fig. 8. Distributions of intra and inter-distances for ICA1 feature vector and single enrollment condition

We have investigated the effect of the training set on the recognition performance. Specifically, we measured the impact of the stress exercises. For example, if the training set consists of hand images under normal conditions but does not contain hands that underwent ice, bag or ball stresses, we could conjecture that the performance would be inferior to the case when these effects are all present in the training set. Thus in the naive set of experiments, we train with N's only but test them with N, B, A and I; in the informed set of experiments, we train with N, B, A and I, and test them also with N, B, A and I.

Similarly we considered the effect of enrollment size, that is, the number of images per subject in the training set. In our case, since we captured three images per subject per session, the enrollment size could be one or two. Consider for example, the three sets of normal condition hands denoted as N1, N2 and N3 (each set has 100 images since there are 100 subjects). The single enrollment consists of querying with the N1 set and searching in the set of 200 images of (N2, N3), (respectively querying with N2 and N3, and searching in the sets, (N1, N3) and (N1, N3). The double enrollment means querying with (N1, N2) and searching in N3 (and the obvious other two combinations). The final result is the average of the three combinations. The performance results for all tests (naive and informed, single and double enrollment) described in Table VI as well as their various fusion combinations are given in Tables IV- XII, Figure V-D and Figure 10. For identification experiments, we provide identification rate;

TABLE VI
THE ORGANIZATION OF THE DATA SETS IN THE EXPERIMENTS FOR ENROLLMENT SIZE AND TRAINING SET

	Sessions	Training Types	Training Size
Naive Tests	Single Enrollment	N	100
	Double Enrollment	N	200
Informed Tests	4× Enrollment	N,B,A,I	400
	8× Enrollment	N,B,A,I	800

for verification experiments, we provide Equal Error Rate (EER) figures and Receiver Operating Characteristics (ROC) curves.

TABLE VII
FUSION RESULTS OF ICA1, LEM AND NMF FOR NAIVE TESTS WITH SINGLE-ENROLLMENT

Test Set	ICA1	Majority V.	Borda C.	Sum	Weighted Sum	Product
Normal	88.66	86.33	86.00	91.16	**93.50**	87.66
Bag	78.33	77.33	79.00	84.66	**85.66**	83.77
Activity	75.55	75.00	76.22	83.33	**84.00**	82.55
Ice	68.77	72.44	73.44	**80.44**	79.77	79.44
All	77.82	77.78	78.67	84.89	**85.73**	83.35

TABLE VIII
FUSION RESULTS OF ICA1, LEM AND NMF FOR NAIVE TESTS WITH DOUBLE-ENROLLMENT

Test Set	ICA1	Majority V.	Borda C.	Sum	Weighted Sum	Product
Normal	94.33	93.00	93.00	**97.33**	**97.33**	93.00
Bag	88.55	88.44	89.88	94.55	**94.77**	92.44
Activity	86.44	87.33	87.55	**92.55**	92.22	91.77
Ice	77.66	82.88	84.77	**90.22**	89.11	89.66
All	86.74	87.91	88.80	**93.66**	93.35	91.71

A. Choice of features

We have observed that ICA1 features almost always had superior performance throughout all the tests, whether naive or informed, single or double enrollment, under normal or adverse conditions. However, despite the lower performance achieved by NMF and LEM features, they still play a useful role when employed in a fusion scheme.

We have considered three score level schemes, one rank level fusion scheme and one decision level fusion scheme to take advantage of the diversity offered by individual feature types. Among the fusion sets of {ICA1, ICA2, NMF, LEM}, {ICA1, NMF, LEM} and {ICA2, NMF, LEM}, the best results were obtained with the {ICA1, NMF, LEM} fusion. Consider, for example, the naive identification test N-versus-NBAI, where the contribution of fusion should be more relevant (Table VII and Table VIII). The improvement brought about by the weighted sum rule is 7.9 points in single enrollment (from 77.8% with ICA1 to 85.7% with fusion), and 7.8 points with double enrollment (from 86.7% with ICA1 to 93.5% with fusion). We found out that the weighted sum rule (with ICA1 weight 0.6, and weights 0.2 to NMF and LEM) brings a slight advantage on average in the naive tests; but SUM rule (all three weights set to 0.33) performs consistently better in the informed tests (TablesX and XII). This indicates that when there are many enrollment images, the simple assumptions made during the computation of the weights do not hold.

Majority voting and Borda count also show improvements under challenging conditions such as ice, but since they are using hard decisions their contributions are not expected as good as the score fusion results. We report majority voting and Borda count performances for the sake of completeness. Product rule fusion improves in most cases the performance vis-a-vis the best performing single feature, though not on a par with the sum rule fusion.

B. Effect of stressors

The effects of adverse conditions created by cold, strong exercise and weight carrying are displayed in Tables VII-VIII and X- XII. We report recognition results for Normal, Bag, Activity and Ice conditions as well as for the case when these four conditions are pooled together (All). As expected, in the naive tests, the performance degrades by 10-20 percentage points. It is interesting to note that ice condition (I) affects the performance more than any other effect. For example, with ICA1 features, if we compare N-to-N results with those of N-to-I results, we observe that naive and single enrollment incurs a drop of 20 points and naive and double enrollment 16.7 points. The drops with the ice condition are less dramatic but still sizeable even with fusion (weighted sum); the losses being 13.7 points and 8.2 points. The message here is that if the test conditions differ from those of training (normal), performance drops are inevitable.

C. Effect of enrollment size

The benefit of multiple enrollments can be read off from these tables. Since we have three images per subject, it is possible to compare only the single and double enrollments. For naive tests and with ICA1 features, the performance improves for N-to-N tests from 88.7% to 94.3% by 6.6 percentage points as we go from single to double enrollment (compare tables IV and V). As another case in point comparison of Tables VII and VIII show that using weighted sum rule, and the N-versus-All test, the performance improves from 85.7% to 93.4% by 7.7 points with the use of double enrollment.

TABLE IX
IDENTIFICATION RATES AND EQUAL ERROR RATES (EER) FOR INFORMED TESTS AND SINGLE ENROLLMENT(4 IMAGES PER SUBJECT, ONE FOR EACH OF N, B, A AND I CONDITIONS)

Test Set		ICA1	ICA2	NMF	LEM
Normal	Iden.Rate:	94.33	**95.33**	92.83	87.66
	EER:	3.71	**1.83**	4.49	5.86
Bag	Iden.Rate:	**91.83**	89.33	90.50	92.00
	EER:	**4.86**	5.79	5.21	**4.18**
Activity	Iden.Rate:	**91.00**	89.16	89.66	92.00
	EER:	**4.98**	5.03	5.50	**4.63**
Ice	Iden.Rate:	**89.50**	87.33	89.50	89.16
	EER:	5.83	4.95	**4.48**	5.51
All	Iden.Rate:	**91.67**	90.29	90.63	90.21
	EER:	**4.85**	**4.41**	4.92	5.05

D. Informed tests versus naive tests

If the classifier is trained with images under normal as well as all possible stressed conditions, the identification and recognition performances definitely improve. In informed tests, the training set consists of normal, bag, activity and ice images, with varying enrollment size. The first observation in Tables IX and XI is that the order of the best performing features is maintained as in the naive tests, so that, with a few insignificant exceptions ICA2 is better when being tested on N's, that is the NBAI-to-N tests, while ICA1 is better in all the remaining conditions. The second observation is that double enrollment brings a significant advantage of 5 percentage points in the overall

TABLE X
FUSION RESULTS OF ICA1, LEM AND NMF FOR THE INFORMED CASE AND SINGLE ENROLLMENT(4 IMAGES PER SUBJECT, ONE FOR EACH OF N, B, A AND I CONDITIONS)

Test Set	ICA1	Majority V.	Borda C.	Sum	Weighted Sum	Product
Normal	94.33	93.83	94.16	**98.16**	97.00	96.33
Bag	91.83	92.50	94.00	**97.16**	96.50	96.16
Activity	91.00	92.16	93.50	**97.66**	97.33	96.66
Ice	89.50	92.50	93.00	**96.83**	96.16	96.00
All	91.67	92.75	93.67	**97.45**	96.74	96.28

TABLE XI
IDENTIFICATION RATES AND EQUAL ERROR RATES (EER) FOR INFORMED TESTS AND DOUBLE ENROLLMENT (8 IMAGES PER SUBJECT, TWO FOR EACH OF N, B, A AND I CONDITIONS)

Test Set		ICA1	ICA2	NMF	LEM
Normal	Iden.Rate:	97.00	**98.66**	96.33	94.33
	EER:	2.29	**1.02**	2.00	3.44
Bag	Iden.Rate:	97.00	94.66	95.00	**98.00**
	EER:	3.31	3.00	3.02	**1.74**
Activity	Iden.Rate:	**98.00**	96.00	96.00	**98.00**
	EER:	**2.94**	2.33	2.37	**2.60**
Ice	Iden.Rate:	94.66	94.33	**95.66**	94.66
	EER:	4.13	2.64	**2.00**	3.39
All	Iden.Rate:	**96.67**	95.92	95.75	96.25
	EER:	3.17	**2.25**	2.35	2.79

TABLE XII
FUSION RESULTS OF ICA1, LEM AND NMF FOR THE INFORMED CASE AND DOUBLE ENROLLMENT (8 IMAGES PER SUBJECT, TWO FOR EACH OF N, B, A AND I CONDITIONS)

Test Set	ICA1	Majority V.	Borda C.	Sum	Weighted Sum	Product
Normal	97.00	97.66	98.00	**99.33**	98.66	97.00
Bag	97.00	95.66	95.00	**99.33**	98.00	99.00
Activity	98.00	76.44	98.33	**100.00**	**100.00**	99.33
Ice	94.66	96.33	98.00	**99.33**	99.00	97.00
All	96.67	91.52	97.33	**99.49**	98.91	98.08

tests, while this advantage amounted to 9 percentage points in the more disadvantaged, hence difficult naive tests (Tables IV and V).The second observation is that using more enrollment images (i.e, 8 instead of 4) brings a significant advantage in the overall tests. The third observation is that feature fusion is advantageous, improving the overall score in the quadruple enrollment case by more than 6 percentage points using Sum Rule (Table X). This result is even better than the fusion advantage in the naive case (2.4 percentage points as in Table VII). The fourth and most important observation is that informed testing, that is, training the classifier with all likely variations to be encountered during testing provides a very significant performance increase; and it is possible to obtain more than 99 percent performance on average with the SUM rule, in the informed case with 8 enrollment images.

E. Factors of Time Lapse, Resolution and Population Size

In this section we investigate the effects of such factors as the time elapsed between the training and test image capture sessions, the way the performance scales with the gallery size, and the imaging resolution.

Part of the database collection process was repeated after three months. Table XIII shows the performance results where Contemporaneous means hand that enrollment and test images were collected within minutes of each other, while Time Lapsed means that a hand presently imaged is tried to be identified and/or verified by considering the hands collected three months ago. A significant drop in performance is observed; pointing to a need for multiple time-lapse enrollment or template adaptation. Figure 10(a) and 10(b) show how EER changes under increasing resolution and increase in gallery size. As expected, performance degrades with decreasing resolution, and increasing gallery size.

TABLE XIII
EFFECTS OF TIME LAPSE DATA (ICA1 NAIVE TESTS)

Version		Contemporaneous	Time Lapsed
Single Enr.	Iden.Rate:	96.00	81.33
	EER:	1.98	9.25
Double Enr.	Iden.Rate:	98.66	88.00
	EER:	0.33	5.02

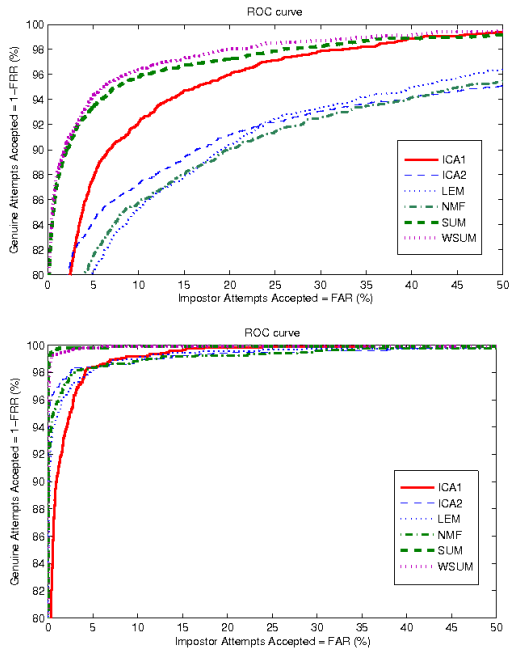

Fig. 9. ROC curves of single enrollment and $8\times$ enrollment

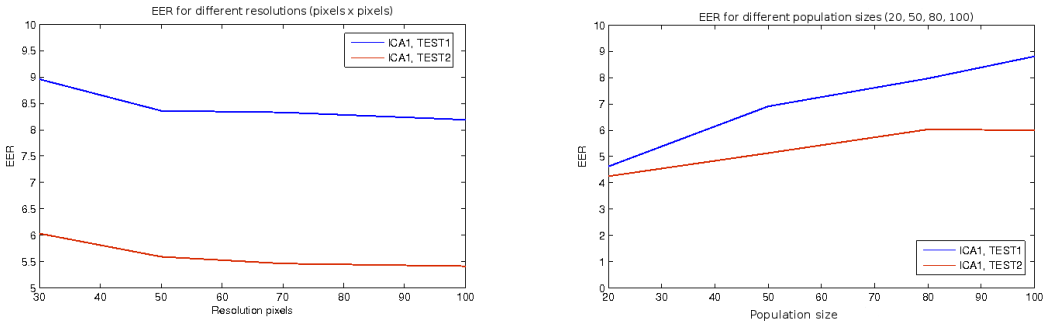

Fig. 10. (a) ICA1, EER performances for different resolutions (30×30, 50×50, 70×70 and 100×100) (b) ICA1, EER performances for different population sizes (20, 50, 80, 100) for naive tests. TEST1 refers to Single Enrollment Tests and TEST2 refers to Double Enrollment Tests that are explained in Table VI

VI. Conclusion

We have collected a hand vein database which we call BOSPHORUS, using near infrared imaging technology, under adverse conditions mirroring real life situations and designed a new biometric identification system based on hand vein patterns. The main novelty of the study is the collection of the BOSPHORUS hand vein database, that includes adversarial conditions, and the study of performance under these conditions. Another contribution is the extensive experimentation on joint appearance-based and geometry-based features. Notice that a variety of different features have recently been analyzed in [27].

The appearance-based features are extracted using ICA and NMF algorithms in this work, and they both have proved superior to the geometry-based LEM technique. Although NMF and LEM are inferior to ICA features alone; their fusion brings significant advantages, pointing out that they provide complementary information. The major conclusions can be summarized as follows:

i. According to the results achieved on the employed dataset, ICA architecture 1 (ICA1) proves to be always slightly better compared to its competitors ICA2, LEM and NMF. Recall that ICA1 presents a parts-based sparse representation while ICA2 gives a holistic view. ICA2 seems to achieve somewhat better results when hands are presented without stressing effects.

ii. For stressed conditions, such as strenuous exercise with the hand, there are large performance drops.
iii. Fusion of the classifier scores under the sum rule improves the performance significantly.

We have shown that hand vein pattern biometry is a promising technique. The BOSPHORUS database is presently publicly available for the sake of reproducable results at http://bosphorus.ee.boun.edu.tr/. Our future research will address several related problems such as: i) Contactless hand vein image acquisition, where the registration and classification are more challenging; ii) The local features of the Gabor, LBP, SIFT or gradient variety; ii) Effects of time lapse analyzed on a more significant volume of subjects.

REFERENCES

[1] Jain, A. K., P. Flynn, and A. A. Ross, Handbook of Biometrics, Springer, 2008.
[2] Ding, Y., D. Zhuang, and K. Wang, A Study of Hand Vein Recognition Method, Proceedings of IEEE International Conference on Mechatronics and Automation, 2005.
[3] Wang, L.-Y., G. Leedham, and D. S.-Y. Cho, Infrared Imaging of Hand Vein Patterns for Biometric Purposes, The Institution of Engineering and Technology, Computer Vision, Vol. 1, pp. 113-122, 2007.
[4] Wang, Z., B. Zhang, W. Chen, and Y. Gao, A Performance Evaluation of Shape and Texture Based Methods for Vein Recognition, Congress on Image and Signal Processing, Vol. 2, pp. 659-661, 2008.
[5] Toh, K.-A., H.-L. Eng, Y.-S. Choo, Y.-L. Cha, W.-Y. Yau, and K.-S. Low, Identity Verification Through Palm Vein and Crease Texture, Lecture Notes in Computer Science, 2005.
[6] Konukoglu, E., E. Yoruk, J. Darbon, and B. Sankur, Shape-Based Hand Recognition, IEEE Transactions on Image Processing, Vol. 15, No. 7, pp. 1803-1815, 2006.
[7] Yoruk, E., H. Dutagaci, and B. Sankur, Hand Biometry, Image and Vision Computing, Vol. 24, No. 5, pp. 483-497, 2006.
[8] Watec, Specifications of the WAT-902H2 ULTIMATE Camera, June 2010, http://www.watec.co.jp/english/bw/wat_902_ultimate.html.
[9] Gao, Y.-S. and M. K. H. Leung, Line Segment Hausdorff Distance on Face Matching, Pattern Recognition, Vol. 35, No. 2, pp. 361-371, February 2002.
[10] Sezgin, M. and B. Sankur, Survey over Image Thresholding Techniques and Quantitative Performance Evaluation, Journal of Electronic Imaging, Vol. 13, No. 1, pp. 146-165, 2004.
[11] Hyvrinen, A. and E. Oja, Independent Component Analysis: Algorithms and Applications, Neural Networks, Vol. 13, No. 4-5, pp. 411-430, 2000.
[12] Gokberk, B., A. A. Salah, and L. Akarun, Rank-Based Decision Fusion for 3D Shape-Based Face Recognition, Audio- and Video-Based Biometric Person Au- thentication (AVBPA), July 2005.
[13] Lin, C.-L. and K.-C. Fan, Biometric Verification Using Thermal Images of Palm- Dorsa Vein Patterns, IEEE Trans. Circuits and Sys. For Video Technology, Vol. 14, No. 2, pp. 199-213, February 2004.
[14] Wang, J.-G., W.-Y. Yau, and A. Suwandy, Fusion of Palmprint and Palm Vein Images for Person Recognition Based on Laplacianpalm Feature, Pattern Recognition, Vol. 41, pp. 1531-1544, May 2008.
[15] Lee, D. D. and H. S. Seung, Algorithms for Non-negative Matrix Factorization, Advances in Neural Information Processing Systems, Vol. 13, pp. 556-562, 2001.
[16] Hoyer, P. O., Non-negative Matrix Factorization with Sparseness Constraints, Journal of Machine Learning Research, Vol. 5, pp. 1457-1469, December 2004.
[17] Zhang, T. Y. and C. Y. Suen, A Fast Parallel Algorithm for Thinning Digital Patterns, Communications of the ACM, Vol. 27, No. 3, pp. 236-239, March 1984.
[18] Weeks, A. R., Fundamentals of Electronic Image Processing, SPIE Press, 1996.
[19] Jain, A. K., L. Hong, S. Pankanti, and R. Bolle, An Identity-Authentication System Using Fingerprints, Proc. IEEE, Vol. 85, No. 9, pp. 1365-1388, September 1997.
[20] Wang, L.-Y., G. Leedham, and D. S.-Y. Cho, Minutiae Feature Analysis for Infrared Hand Vein Pattern Biometrics, The Journal of the Pattern Recognition Society, Vol. 41, No. 3, pp. 920-929, March 2008.
[21] Lecornu, L., C. Roux, and J. Jacque, Extraction of Vessel Contours in Angiograms by Simultaneous Tracking of the Two Edges, IEEE Conf. Eng. in Medicine and Bio., Vol. 1, pp. 678-679, 1994.
[22] Martelli, A., An Application of Heuristic Search Methods to Edge and Contour Detection, Comm. ACM, Vol. 19, pp. 73-83, 1976.
[23] Luo, H., F. Yu, J. Pan, S. Chu, and P. Tsai, A Survey of Vein Recognition Techniques, Information Technology Journal, Vol. 9, No. 6, pp. 1142-1149, 2010.
[24] Stan, Z. Li. (Editor), Encyclopedia of Biometrics, Vol. 2, Springer, 2009.
[25] Ekenel, H., K. and B. Sankur, Feature selection in the independent component subspace for face recognition, Pattern Recognition Letters, Vol. 23, pp. 1377-1388, 2004.
[26] Dutagaci, H., B. Sankur, and E. YorukA comparative analysis of global hand appearance based person recognition, J. Electronic Imaging, Vol. 17, No.1, 011018/1- 011018/19, 2008.
[27] Kumar, A., K. and K., V. Prathyusha, Personal authentication using hand vein triangulation, IEEE Trans. Image Process., Vol. 38, pp. 2127-2136, 2009.
[28] Zhou, Y., K. and A. Kumar, Contactless palmvein identification using multiple representations, Proc. BTAS 10, Washington, D.C., 2010.